A 0.5–4.0-GHz Tunable Bandpass Filter Using YIG Film Grown by LPE

YOSHIKAZU MURAKAMI, TAKAHIRO OHGIHARA, AND TSUTOMU OKAMOTO

Abstract—A tunable bandpass filter using YIG film grown by liquid phase epitaxy (LPE) has been developed. Taking advantage of the very low resonance frequency in the perpendicular resonance of YIG film, an operation frequency of 0.5 GHz has been achieved. In order to make this filter operate up to 4.0 GHz, a new technique for multioctave tuning has been developed and applied to the filter. Over the wide tuning range from 0.5 GHz to 4.0 GHz, low insertion loss and high spurious suppression have been achieved. The performance of this filter satisfies the requirements for use as a tracking preselector in a microwave spectrum analyzer.

I. Introduction

YTTRIUM IRON GARNET (YIG) grown as bulk single crystals and fabricated into highly polished spheres is commonly used in microwave filters and oscillators which are electronically tunable over a wide frequency range. Although these filters and oscillators have excellent characteristics, their construction involves precision processes which cause their cost to be high and limit their application to sophisticated systems. In contrast, high-quality YIG film grown by LPE can be used to construct devices in a microwave integrated circuit (MIC) format at a moderate cost [1]. Furthermore, in the perpendicular resonance of YIG film, the resonance starts from a much lower frequency than in a YIG sphere. These advantages make YIG film devices covering a low-frequency range below 1 GHz highly competitive with the YIG sphere devices.

Although considerable work has been done on magnetostatic-wave (MSW) devices utilizing YIG film, a persistent problem is the high insertion loss of these devices when applied to microwave bandpass filters [2], [3]. We have previously reported a 1.575-GHz fixed-frequency bandpass filter using the uniform precession mode of perpendicular resonance of YIG film to achieve a low insertion loss [4]. Forming a circular groove on the surface of the YIG disk allowed us to solve the inherent problem of spurious responses due to higher order magnetostatic modes, and a high spurious suppression has been achieved.

This paper describes the application of this technique to a low-frequency tunable bandpass filter used as a tracking preselector in a microwave spectrum analyzer. The low-frequency limit of the resonance in YIG films was investigated in order to obtain a high unloaded Q even at frequencies below 1 GHz. The fabrication of the filter achieving the very low operation frequency of 0.5 GHz will be described. The equivalent circuit of the two-stage filter was analyzed to obtain the limiting factor of the useful tuning range. A new design approach for multioctave YIG-tuned filters (YTF) which expands the present filter's operation frequency up to 4.0 GHz will also be described.

Manuscript received March 13, 1987; revised July 13, 1987.

The authors are with the Sony Corporation Research Center, 174 Fujitsuka-cho, Hodogaya-ku, Yokohama, 240 Japan.

IEEE Log Number 8717110.

II. Device Fabrication

The configuration of the two-stage filter is shown in Fig. 1. Two YIG disk resonators were fabricated from lanthanum-substituted yttrium iron garnet (La:YIG) film epitaxially grown on a (100) gadolinium gallium garnet (GGG) substrate. Lanthanum was substituted to match the lattice constant of YIG film with that of the GGG substrate. A (100) YIG film was chosen in order to obtain a resonance frequency limit as low as possible and to obtain a higher unloaded Q than with film otherwise oriented, especially in the low-frequency range below 1 GHz. A grooved circle concentric with the center of the disk was formed photolithographically on the surface of the disk [4]. The position of the groove was calculated using magnetostatic mode theory at the node of the uniform precession mode of perpendicular resonance [5]. Here the RF magnetization of the higher order magnetostatic modes of perpendicular resonance has a finite amplitude. Hence, as the magnetization is pinned at the groove, suppression of the higher order magnetostatic modes is achieved. As this spurious suppression technique is based on magnetostatic mode theory, it has intrinsic broad-band characteristics and works efficiently for a tunable filter. The disks were 2.5 mm in diameter and 40 μm thick. The distance between the centers of the disks was 5 mm.

Input, output, and interresonator coupling striplines were formed photolithographically on a quartz substrate. The interresonator coupling stripline was grounded at both ends in the conventional manner. The ends of the input and output striplines were grounded via narrow portions which were bent 90°, thus limiting the direct coupling between the input and output striplines generated by the RF magnetic field and improving the filter's isolation characteristics.

A shielded suspended stripline structure was adopted because of the following advantages:

1) The RF electromagnetic field is not disturbed by external conductors such as a magnetic yoke or coils.

0018-9480/87/1200-1192$01.00

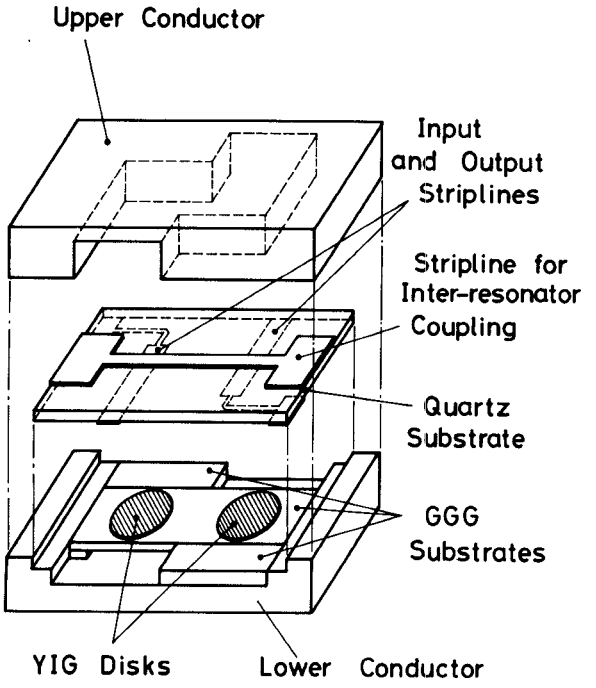

Fig. 1. Configuration of the two-stage filter.

2) The width of the 50-Ω stripline is kept wide in order to make the electromagnetic coupling to the YIG disk resonator strong and, together with the grooved circle, to improve spurious suppression.
3) The two additional air gaps of this structure and the fact that the striplines can be positioned either above, below, or between the dielectric substrates give much greater flexibility in determining the structure parameters which will optimize the strength of the couplings.

A biasing magnetic field of about 1910 Oe for 0.5 GHz and 3160 Oe for 4.0 GHz was applied perpendicularly by a tuning magnet.

III. Low-Frequency Limit of Resonance

The low-frequency limit of the resonance in YIG is determined by two factors: the effect of demagnetization and the magnetocrystalline anisotropy. For a YIG spheroid immersed in an uniform axial magnetic field H_0, the internal field H_i is given by

$$H_i = H_0 - N_z 4\pi M_s \tag{1}$$

where N_z is the axial demagnetizing factor and $4\pi M_s$ is the saturation magnetization. The resonance frequency of the YIG spheroid is given by Kittel's equation:

$$\begin{aligned}\omega &= \gamma\{H_0 - (N_z - N_t)4\pi M_s\} \\ &= \gamma(H_i + N_t 4\pi M_S)\end{aligned} \tag{2}$$

where γ is the gyromagnetic ratio and N_t is the transverse demagnetization factor. For low-loss resonance, the ferrimagnetic sample must be saturated and the internal magnetic field H_i must be positive. Hence, the minimum resonance frequency is

$$\omega_{\min} = \gamma N_t 4\pi M_s. \tag{3}$$

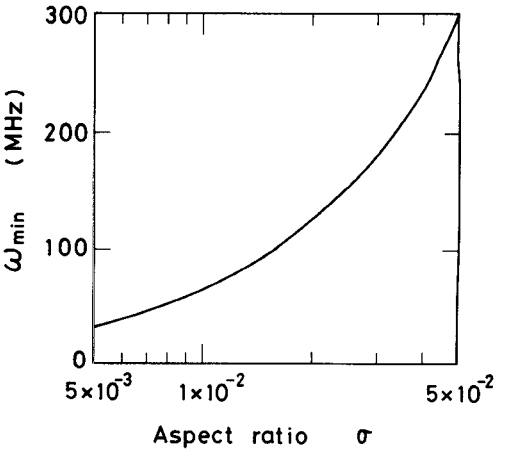

Fig. 2. Calculated $\omega_{\min}$ from the effect of demagnetization.

For a pure YIG sphere, $N_t = 1/3$, and $\omega_{\min}$ is about 1.6 GHz.

As a disk is not strictly ellipsoidal, the internal magnetic field becomes nonuniform and takes the minimum value

$$H_i' = H_0 - N_z' 4\pi M_s \tag{4}$$

at the center of the disk. The resonance frequency of the uniform precession mode of the YIG disk can be calculated from the magnetostatic mode theory and expressed by Kittel's equation (2) [5]. From (2) and (4), the minimum resonance frequency can be written as

$$\begin{aligned}\omega_{\min} &= \gamma\{N_z' - (N_z - N_t)\}4\pi M_s \\ &= \gamma N_t' 4\pi M_s\end{aligned} \tag{5}$$

where N_t' depends only on its aspect ratio σ (thickness/diameter). Fig. 2 shows the $\omega_{\min}$ calculated from the magnetostatic mode theory for $4\pi M_s = 1800$ G.

Cubic crystal anisotropy and uniaxial anisotropy are responsible for the magnetocrystalline anisotropy in an epitaxial YIG film. When the external magnetic field is applied perpendicularly, the resonance frequency in (100) and (111) YIG films can be expressed as

$$\omega = \gamma(H_0 + 2K_u/M_s - 2|K_1|/M_s)$$

for (100) YIG film and $H_0 > 2|K_1|/M_s - 2K_u/M_s$ (6)

and

$$\omega = \gamma(H_0 + 2K_u/M_s + 4|K_1|/3M_s) \quad \text{for (111) YIG film} \tag{7}$$

where K_1 is the first-order constant of cubic anisotropy and is negative for YIG, and K_u is the uniaxial anisotropy constant [6]. With the substitution of lanthanum to match the lattice constant of YIG film to that of the GGG substrate, the uniaxial anisotropy is sufficiently reduced. When this is the case, the overall low-frequency limit of resonance becomes

$$\omega_{\min} = \gamma N_t' 4\pi M_s \quad \text{for (100) YIG disk} \tag{8}$$

and

$$\omega_{\min} = \gamma(N_t' 4\pi M_s + 4|K_1|/3M_s) \quad \text{for (111) YIG disk.} \tag{9}$$

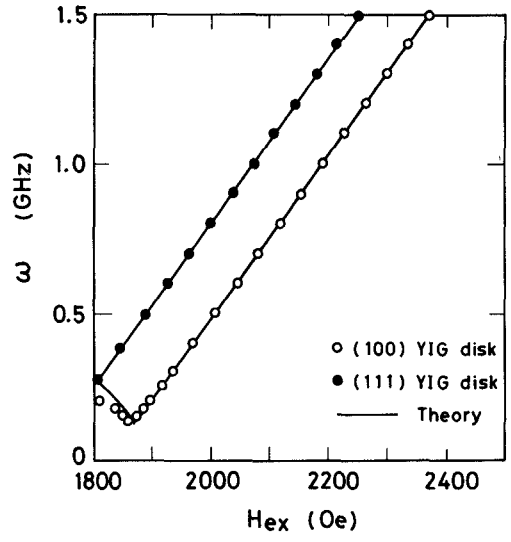

Fig. 3. Resonance frequency plotted against the external magnetic field.

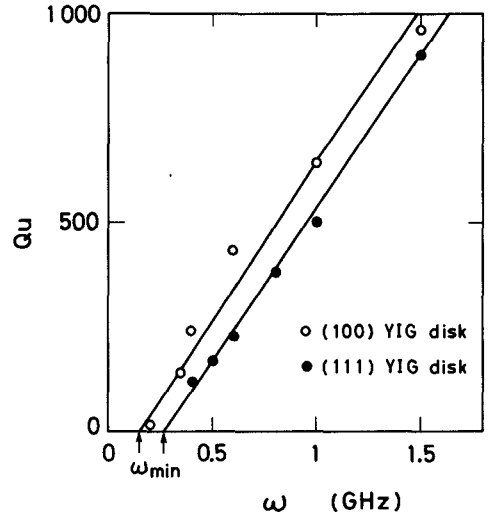

Fig. 4. Q_u plotted against the resonance frequency.

Next, the low-frequency limits of the perpendicular resonance in (100) and (111) YIG disks, which were 2.5 mm in diameter and 50 μm thick, were measured from the bandstop configurations and compared to the theoretical predictions. Fig. 3 shows the variation of the resonance frequency with the change of externally applied field measured for each YIG disk, and the solid lines in the figure are theoretical curves. The minimum resonance frequencies observed in (100) and (111) YIG disks were 140 MHz and 270 MHz, respectively, which agrees very well with the theoretical values of 125 MHz and 274 MHz calculated from (8) and (9). Fig. 4 shows the measured plots of the unloaded Q of the YIG disk resonator against the resonance frequency. From this, the unloaded Q can be expressed as

$$Q_u = (\omega - \omega_{\min})/\gamma \Delta H \tag{10}$$

where ΔH is the resonance line width. Based on the above, we can now understand that, for YIG devices operating in the frequency range below 1 GHz, it is preferable to use the perpendicular resonance in a (100) YIG disk where the frequency limit of resonance is very low.

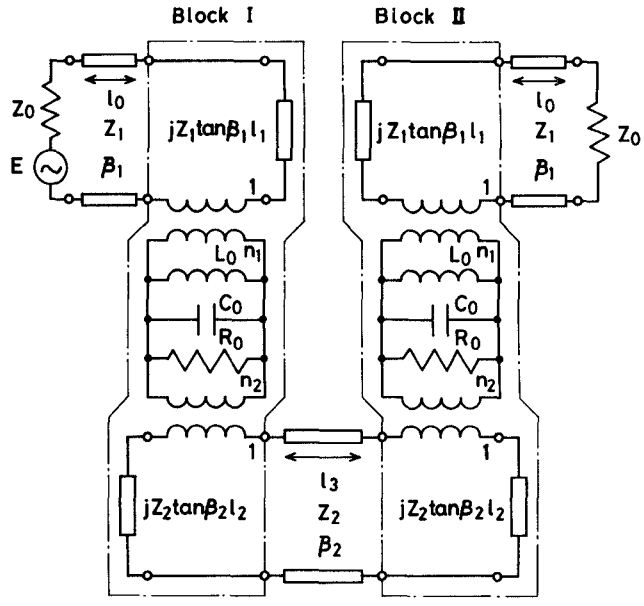

Fig. 5. Equivalent circuit of the line-coupled two-resonator filter.

IV. Design of the Multioctave YTF

The equivalent circuit of the two-stage filter shown in Fig. 5 was analyzed to obtain the coupling coefficient k between the two YIG disk resonators. The S parameters of block I can be written as follows:

$$S_{11}^{\mathrm{I}} = \frac{(-1 + j\tan\beta_1 l_1)\left\{\frac{1}{Q_u} + \frac{1}{Q_{e2}(1 + j\tan\beta_2 l_2)} + j\Omega\right\} + \frac{1}{Q_{e1}}}{(1 + j\tan\beta_1 l_1)\left\{\frac{1}{Q_u} + \frac{1}{Q_{e2}(1 + j\tan\beta_2 l_2)} + j\Omega\right\} + \frac{1}{Q_{e1}}}$$

$$S_{21}^{\mathrm{I}} = S_{12}^{\mathrm{I}} = \frac{2}{\frac{\sqrt{Q_{e1}Q_{e2}(1 + j\tan\beta_1 l_1)(1 + j\tan\beta_2 l_2)}}{\frac{1}{Q_u} + \frac{1}{Q_{e1}(1 + j\tan\beta_1 l_1)} + \frac{1}{Q_{e2}(1 + j\tan\beta_2 l_2)} + j\Omega}}$$

$$S_{22}^{\mathrm{I}} = \frac{(-1 + j\tan\beta_2 l_2)\left\{\frac{1}{Q_u} + \frac{1}{Q_{e1}(1 + j\tan\beta_1 l_1)} + j\Omega\right\} + \frac{1}{Q_{e2}}}{(1 + j\tan\beta_2 l_2)\left\{\frac{1}{Q_u} + \frac{1}{Q_{e1}(1 + j\tan\beta_1 l_1)} + j\Omega\right\} + \frac{1}{Q_{e2}}} \tag{11}$$

where β_1 and β_2 are the phase constants of the input/output stripline and the interresonator stripline, respectively, l_1 and l_2 are the distances from the center of the disk to the shorted ends of the input/output stripline and the interresonator stripline, respectively, $\Omega = \omega/\omega_0 - \omega_0/\omega$, $\omega_0 = 1/\sqrt{L_0 C_0}$ is the resonance angular frequency, Q_u is the unloaded Q of the resonator, and $Q_{e1} = n_1^2 Z_1 \omega_0 C_0$ and $Q_{e2} = n_2^2 Z_2 \omega_0 C_0$ are the external Q's. As the filter is symmetrical, the S parameters of block II are related to the S parameters of block I as

$$\begin{aligned} S_{11}^{\mathrm{II}} &= S_{22}^{\mathrm{I}} \\ S_{21}^{\mathrm{II}} &= S_{12}^{\mathrm{II}} = S_{21}^{\mathrm{I}} \\ S_{22}^{\mathrm{II}} &= S_{11}^{\mathrm{I}}. \end{aligned} \tag{12}$$

Then, the elements of the overall S matrix, (S^L), of the cascaded two-port networks from block I to block II are obtained as

$$S_{11}^L = S_{22}^L = \frac{S_{11}^{\mathrm{I}} + \left\{\left(S_{21}^{\mathrm{I}}\right)^2 - S_{11}^{\mathrm{I}} S_{22}^{\mathrm{I}}\right\} S_{22}^{\mathrm{I}} \exp\left(-2j\beta_2 l_3\right)}{1 - \left(S_{22}^{\mathrm{I}}\right)^2 \exp\left(-2j\beta_2 l_3\right)}$$

$$S_{21}^L = S_{12}^L = \frac{\left(S_{21}^{\mathrm{I}}\right)^2 \exp\left(-j\beta_2 l_3\right)}{1 - \left(S_{22}^{\mathrm{I}}\right)^2 \exp\left(-2j\beta_2 l_3\right)} \tag{13}$$

where l_3 is the distance between the centers of the disks.

Substituting (11) into (13), the expressions for the S_{ij}^L's are obtained as follows:

$$S_{11}^L = S_{22}^L = -\exp\left(-2j\beta_1 l_1\right) \cdot \frac{\left(\frac{1}{Q_u} + \frac{\cos^2\beta_1 l_1}{Q_{e1}} + j\Omega'\right)\left(\frac{1}{Q_u} - \frac{\cos^2\beta_1 l_1}{Q_{e1}} + j\Omega'\right) + \left\{\frac{\cos^2\beta_2 l_2}{Q_{e2}\sin\beta_2(2l_2 + l_3)}\right\}^2}{\left(\frac{1}{Q_u} + \frac{\cos^2\beta_1 l_1}{Q_{e1}} + j\Omega'\right)^2 + \left\{\frac{\cos^2\beta_2 l_2}{Q_{e2}\sin\beta_2(2l_2 + l_3)}\right\}^2}$$

$$S_{21}^L = S_{12}^L = \exp - j(2\beta_1 l_1 + \pi/2) \cdot \frac{2\left\{\frac{\cos^2\beta_2 l_2}{Q_{e2}\sin\beta_2(2l_2 + l_3)}\right\}\left(\frac{\cos^2\beta_1 l_1}{Q_{e1}}\right)}{\left(\frac{1}{Q_u} + \frac{\cos^2\beta_1 l_1}{Q_{e1}} + j\Omega'\right)^2 + \left\{\frac{\cos^2\beta_2 l_2}{Q_{e2}\sin\beta_2(2l_2 + l_3)}\right\}^2} \tag{14}$$

where $\Omega' = \omega/\omega_0' - \omega_0'/\omega$, $\omega_0' = \omega_0 + \Delta\omega_0$, and

$$\Delta\omega_0 = \frac{\omega_0}{2}\left\{\frac{\sin 2\beta_1 l_1}{2Q_{e1}} + \frac{\cos\beta_2 l_2 \cos\beta_2(l_2 + l_3)}{Q_{e2}\sin\beta_2(2l_2 + l_3)}\right\} \tag{15}$$

represents the difference between the filter's center frequency and the resonance frequency of YIG disks.

Now let us consider the equivalent circuit of the direct-coupled two-resonator filter shown in Fig. 6 [7]. The elements of the S matrix, (S^D), are obtained as

$$S_{11}^D = S_{22}^D = -\frac{\left(\frac{1}{Q_u} + \frac{1}{Q_{e,i/o}} + j\Omega\right)\left(\frac{1}{Q_u} - \frac{1}{Q_{e,i/o}} + j\Omega\right) + k^2}{\left(\frac{1}{Q_u} + \frac{1}{Q_{e,i/o}} + j\Omega\right)^2 + k^2}$$

$$S_{21}^D = S_{12}^D = \frac{\frac{2k}{Q_{e,i/o}}}{\left(\frac{1}{Q_u} + \frac{1}{Q_{e,i/o}} + j\Omega\right)^2 + k^2}. \tag{16}$$

Comparing (14) with (16), it is seen that the S matrix, (S^L), of the line-coupled two-resonator filter coincides with the S matrix, (S^D), of the direct-coupled two-resonator filter except for the additional phase terms of $\exp(-2j\beta_1 l_1)$ and $\exp - j(2\beta_1 l_1 + \pi/2)$. It is also seen that the coupling coefficient k between the two YIG disk resonators and the input and output external $Q, Q_{e,i/o}$, can be expressed as

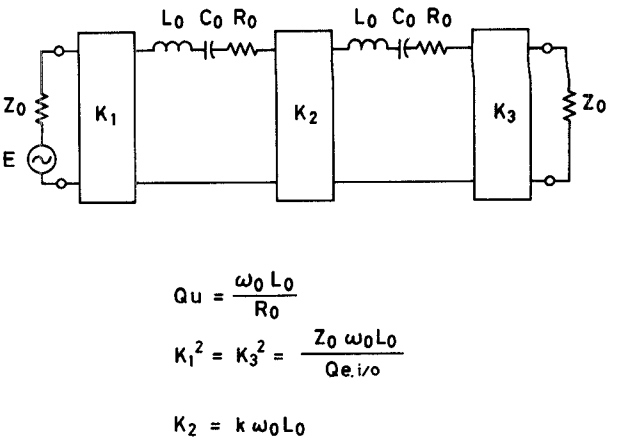

Fig. 6. Equivalent circuit of the direct-coupled two-resonator filter.

$$k = \frac{\cos^2(\beta_2 l_2)}{Q_{e2}\sin(\beta_2 l_c)} \tag{17}$$

and

$$Q_{e,i/o} = \frac{Q_{e1}}{\cos^2\beta_1 l_1} \tag{18}$$

where $l_c = 2l_2 + l_3$ is the length of the stripline for interresonator coupling. When both ends of the stripline for interresonator coupling are grounded at the edge of each YIG disk, as it is in this case, l_2 is sufficiently small, and (17) can be approximated as

$$k = \frac{V_c}{Q_{e2} 2\pi f \sqrt{\epsilon_{\mathrm{eff}}}\, l_c} \tag{19}$$

where V_c is the velocity of light, and ϵ_{eff} is the effective dielectric constant of the stripline for interresonator coupling. From (19), it can be seen that k is inversely proportional to frequency. When the perpendicular resonance of a (100) YIG disk whose aspect ratio σ is about 1.6×10^{-2}

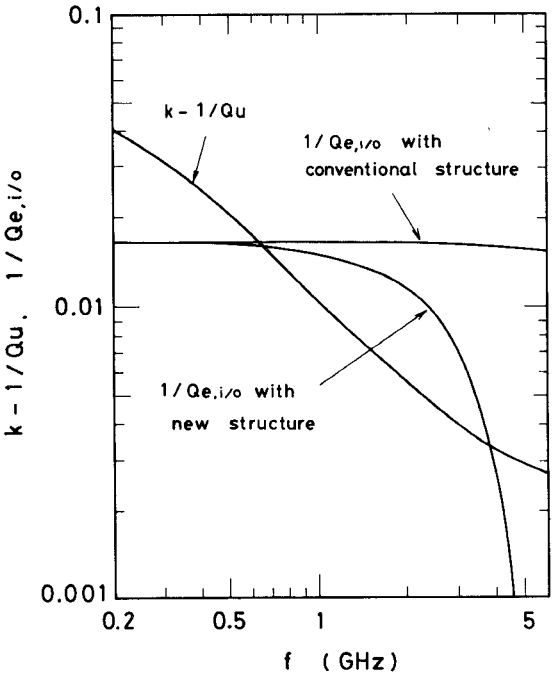

Fig. 7 Frequency dependence of $k-1/Q_u$ and $1/Q_{e,i/o}$.

is used, $\omega_{\min}$ is as low as 100 MHz, and from (10), the unloaded Q of the YIG resonator is approximately proportional to frequency. Consequently, the value of $k-1/Q_u$ is approximately inversely proportional to frequency, as is shown in Fig. 7.

When the ends of input and output striplines are also grounded at the edge of each YIG disk, as is commonly done, the external Q remains approximately constant from (18), as is shown in Fig. 7, so the filter is overcoupled at the lower frequency of the tuning range and undercoupled at the higher frequency of the tuning range, thus limiting the useful tuning range of the filter. Fig. 8 shows the change of the filter's characteristics with frequency as obtained by simulation and experiment. As is seen from the figure, the performance of the filter degrades at both ends of the tuning range.

The ends of the input and output striplines were extended beyond the edge of the YIG disk. Then, from (18), the external Q has the following frequency dependence:

$$Q_{e,i/o}=\frac{Q_{el}}{\cos^2(\beta_1 l_1+\beta_{xl}l_{xl})} \tag{20}$$

where β_{xl} is the phase constant of the extended portion of the stripline, and l_{xl} is the length extended. Now, the critically coupled condition

$$k\sim\frac{1}{Q_u}+\frac{1}{Q_{e,i/o}} \tag{21}$$

can be essentially realized in the wide frequency range, as is shown in Fig. 7.

Fig. 9 compares the results of the simulation and the experiment of the filter with line extension. The maximum operation frequency was extended to 4.0 GHz in this structure, compared with 2.0 GHz in the conventional

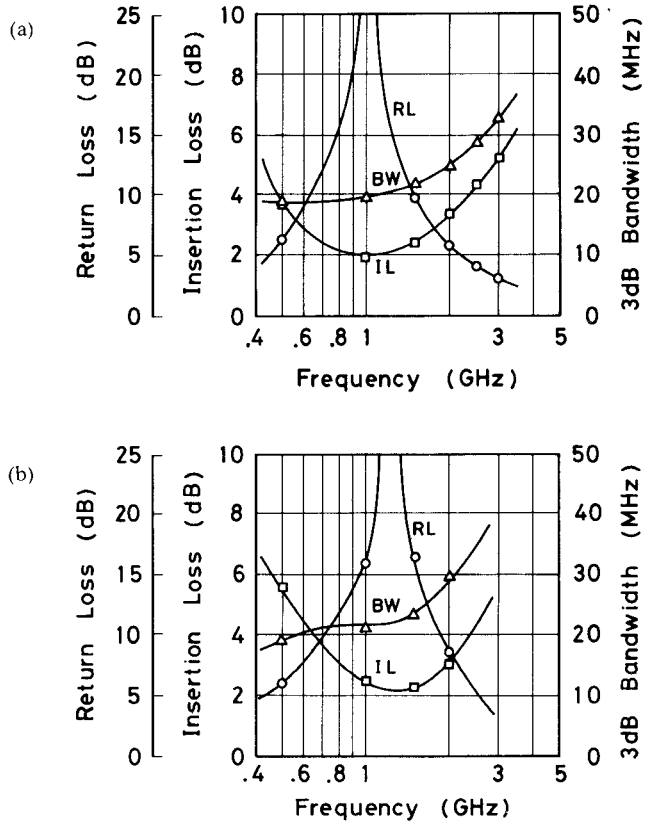

Fig. 8. Frequency dependence of insertion loss, return loss, and 3-dB bandwidth of the filter with the conventional structure. (a) Simulation. (b) Experiment

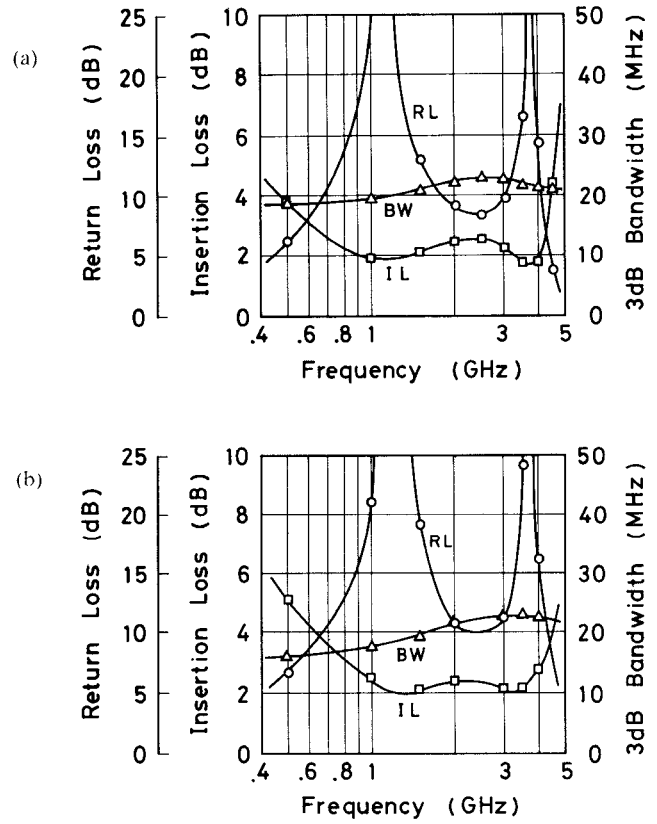

Fig. 9 Frequency dependence of insertion loss, return loss, and 3-dB bandwidth of the filter with the new structure (a) Simulation. (b) Experiment

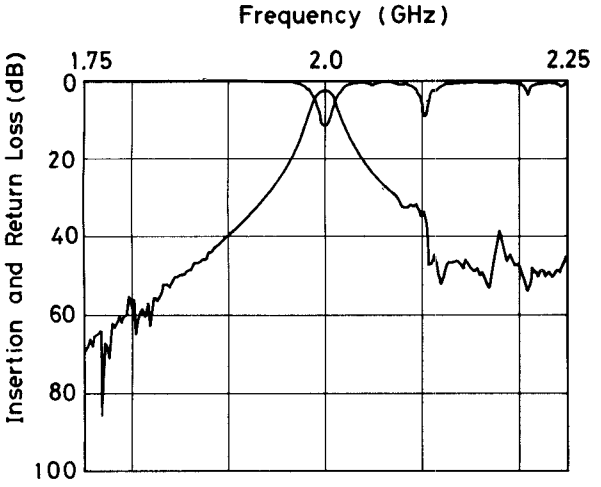

Fig. 10 Transmission and reflection response of the new filter at 2 GHz.

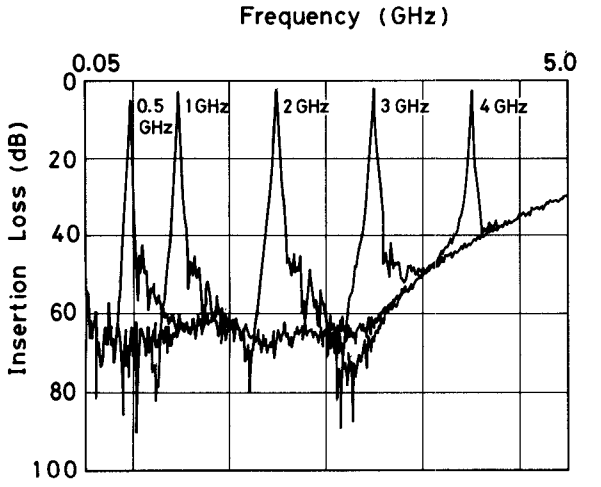

Fig. 11 Transmission response of the new filter when tuned from 0.5 GHz to 4.0 GHz

structure. This broad-band technique has the following advantages:

1) The spurious responses of the filter become relatively strong when the filter is undercoupled. As the filter is essentially critically coupled in the wide center portion of the tuning range and overcoupled at both ends of the tuning range, it serves to improve spurious suppression.
2) As both the external $Q, Q_{e,i/o}$, and the inverse of the coupling coefficient k are approximately proportional to frequency, the 3-dB bandwidth of the filter remains constant.

V. Performance

Fig. 10 shows the typical transmission and reflection response of the filter measured at 2 GHz, the mid-frequency of the tuning range. Fig. 11 shows the change of the transmission response when the filter is tuned from 0.5 GHz to 4.0 GHz. The characteristics of the filter are summarized in Table I. A low insertion loss of less than 3 dB except at 0.5 GHz and a high spurious suppression of more than 35 dB have been achieved. The limiting level of the filter is 0 dBm even at the lowest frequency of 0.5 GHz. This limiting level is substantially higher than that of YIG sphere filters operating in this frequency range. This is because in YIG spheres low-level coincident limiting occurs with power levels of -20 dBm at frequencies below $(2/3)\gamma 4\pi M_s$, which is 3.3 GHz in pure YIG [8]. In contrast, coincident limiting does not occur in the perpendicular resonance of YIG disks. This is another advantage of filters using the perpendicular resonance of a YIG film.

TABLE I
Characteristics of the 0.5–4.0 GHz Tunable Bandpass Filter

Frequency range (GHz)	0.5 - 4.0
Insertion loss (dB)	2.0 - 2.8 (1.0 - 4.0 GHz) 5.0 (at 0.5 GHz)
Return loss (dB)	> 10 (1.0 - 4.0 GHz) 6.7 (at 0.5 GHz)
3dB bandwidth (MHz)	16 - 23
Isolation (dB)	> 50 (≤ 3.5 GHz) 43 (at 4.0 GHz)
Off-resonance spurious(dB)	> 35
Limiting level (dBm)	< 0

VI. Conclusions

A 0.5–4.0-GHz tunable bandpass filter using YIG film grown by LPE has been developed. A technique for designing the multioctave YTF has been developed and applied to the filter. Low insertion loss and high spurious suppression have been achieved, and the performance of this filter satisfies the requirements for use as a tracking preselector in a microwave spectrum analyzer. It has been possible for the first time to take advantage of the very low resonance frequency of YIG film to realize a low-frequency preselector filter.

Acknowledgment

The authors wish to thank Miss K. Niikura for her contributions. They also thank Dr. T. Yamada for encouragement.

References

[1] J. D. Adam, J. H. Collins, and J. M. Owens, "Microwave device applications of epitaxial magnetic garnets," *Radio Electron. Eng.*, vol. 45, no. 12, pp. 738–748, 1975.
[2] J. P. Castera and P. Harteman, "A multipole magnetostatic volume wave resonator filter," *IEEE Trans. Magn.*, vol. MAG-18, pp. 1601–1603, 1982.
[3] E. Huijer and W. Ishak, "MSSW Resonators with Straight Edge Reflectors," *IEEE Trans. Magn.*, vol. MAG-20, pp. 1232–1234, 1984.
[4] Y. Murakami and S. Itoh, "A 1.575 GHz bandpass filter using YIG film grown by LPE," in *IEEE MTT-S Int. Microwave Symp. Dig.*, 1985, pp. 285–287.

[5] Y. Ikusawa and K. Abe, "Resonant modes of magnetostatic waves in a normally magnetized disk," *J. Appl. Phys.*, vol. 48, no. 7, pp. 3001–3007, July 1977.
[6] B. Lax and K. J. Button, *Microwave Ferrites and Ferrimagnetics*. New York: McGraw-Hill, 1962.
[7] G. L. Matthaie, L. Young, and E. M. T. Jones, *Microwave Filters, Impedance Matching Networks and Coupling Structures*. New York: McGraw-Hill, 1964.
[8] J. Helszajn, *YIG Resonators and Filters*, Chichester, England: Wiley, 1985.

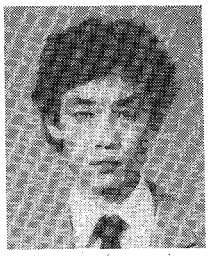

Takahiro Ohgihara was born in Hokkaido, Japan, in 1950. He received the B.S. and M.S. degrees in applied physics from Hokkaido University, Japan, in 1983 and 1985, respectively.

He joined the Sony Corporation Research Center in 1985, and has been engaged in research on microwave integrated circuits. He is currently engaged in the development of microwave filters and oscillators using epitaxial yttrium iron garnet film.

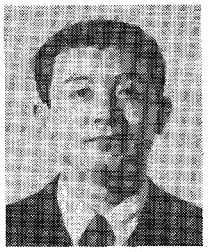

Yoshikazu Murakami was born in Aichi, Japan, in 1950. He received the B.S. degree in physics from Nagoya University, Japan, in 1973.

In 1974, he joined the Sony Corporation Research Center, Yokohama, Japan. He has been engaged in research on microwave integrated circuits. He is currently engaged in the development of microwave filters and oscillators using epitaxial yttrium iron garnet film.

Mr. Murakami is a member of the Institute of Electronics, Information and Communication Engineers of Japan.

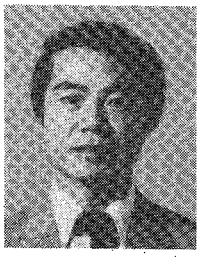

Tsutomu Okamoto was born in Shizuoka, Japan, in 1948.

In 1966, he joined the Sony Corporation Research Center, and has been involved in research on dielectric and magnetic materials. He has been engaged in the development of bismuth germanate single crystal and cobalt nickel magnetic alloy. He is currently engaged in the growth of epitaxial yttrium iron garnet film and magnetic metal crystals.